

# Cramér-Rao Bound Analysis of Echo Time Selection for $^1\text{H}$ -MR Spectroscopy

Hien M. Nguyen, Zhubin J. Gahvari, Justin P. Haldar, Minh N. Do, and Zhi-Pei Liang

**Abstract**—The choice of echo time (TE) is a complicated and controversial issue in proton MR spectroscopy, and represents a balancing act between signal-to-noise ratio and signal complexity. The TE values used in previous literature were selected either heuristically or based on limited empirical studies. In this work, we reconsider this problem from an estimation theoretic perspective. Specifically, we analyze the Cramér-Rao lower bound on estimated spectral parameters as a function of TE, which serves as a metric to quantify the reliability of the estimation procedure. This analysis reveals that a good choice of TE often depends on the particular metabolite of interest, and is a function of both the coupling properties of the metabolites and the general complexity of the spectrum.

## I. INTRODUCTION

Magnetic resonance (MR) spectroscopy enables the non-invasive differentiation and quantitation of different chemical compounds. In proton ( $^1\text{H}$ ) MR spectroscopy,  $^1\text{H}$  nuclei in different molecular environments resonate at different frequencies in the presence of an externally applied magnetic field. This phenomenon can be manipulated to form a spectrum, from which one can study the *in vivo* metabolism of biological tissues.

In MR experiments, the *echo time* (TE) is an important timing parameter that effects the signal-to-noise ratio (SNR), the number of metabolites that contribute significantly to the observed data, the complexity of the spectral baseline, and the spectral profile of each individual metabolite. All of these factors affect the interpretation of the observed spectrum to varying degrees, and the choice of TE remains controversial [1]. In particular, shorter TE spectra generally have higher SNR and contain significant contributions from a larger number of metabolites than long TE spectra; however, this advantage can be offset by the more complicated signal model that must be used to describe short TE data.

In the existing literature, the TE parameter was often chosen based on qualitative metrics, such as the visual characteristics of the spectrum, or to be consistent with previous studies. Some quantitative empirical comparisons between short and long TE spectra have been reported in [2]–[4], though these studies only investigate up to three different TEs.

In this paper, we consider the choice of TE from an estimation theoretic perspective. Specifically, we analyze the Cramér-Rao lower bound (CRB) on the variance of the

metabolite amplitude estimates as a function of TE. While retrospective use of the CRB is common in MR spectroscopy as a metric of quality for an acquired experimental dataset [5]–[7], we are interested in using the CRB prospectively to guide the design of an experiment. This new approach provides a method for identifying potentially useful TEs from an arbitrarily large range of candidate values.

## II. SPECTRAL MODEL AND CRAMÉR-RAO BOUND EXPRESSION

### A. Model formulation

The observed discrete signal from a system with  $N$  spectral components can be modeled as the following:

$$\begin{aligned} s[m] &= \sum_{n=1}^N a_n(TE) e^{j\phi_0} \varphi_{n,TE}[m] \psi_{n,r_n}[m] + \xi[m], \\ m &= 0, \dots, M-1. \end{aligned} \quad (1)$$

Each spectral component is characterized by the real, positive amplitude  $a_n(TE)$ , known metabolite basis function  $\varphi_{n,TE}[m]$ , and the signal decay  $\psi_{n,r_n}[m]$ , where  $r_n$  denotes a lineshape parameter. In addition, the model includes a zero-order phase term  $\phi_0$  for the whole spectrum, and  $\xi[m]$  denotes additive noise.

As TE increases, the amplitudes  $a_n(TE)$  decrease due to spin relaxation, leading to a reduction in SNR. In this work, we assume exponential decay such that

$$a_n(TE) = c_n e^{-TE/T_{2,n}}, \quad (2)$$

where  $T_{2,n}$  is a metabolite-dependent relaxation constant.

The basis functions  $\varphi_{n,TE}[m]$  can change with TE due to quantum mechanical effects, and, as we will see later, this plays an important role in the behavior of the CRB as a function of TE. We assume that the basis function is known and has the form

$$\varphi_{n,TE}[m] = \sum_{l=1}^{L_n} \alpha_{l,n}(TE) e^{j\beta_{l,n}(TE)} e^{j2\pi f_{l,n}(TE)m\Delta_t}, \quad (3)$$

where  $\Delta_t$  denotes the sampling time and  $\alpha_{l,n}(TE)$ ,  $\beta_{l,n}(TE)$ , and  $f_{l,n}(TE)$  are the relative amplitude, phase, and frequency of the  $l$ -th resonance, belonging to the  $n$ -th metabolite. These parameters can be obtained from quantum mechanical simulations.

In addition, we model the signal decay of each spectral component as Lorentzian

$$\psi_{n,r_n}[m] = e^{-m\Delta_t/r_n}, \quad (4)$$

H. Nguyen, Z. Gahvari, J. Haldar, M. Do, and Z.-P. Liang are with the Department of Electrical and Computer Engineering, University of Illinois at Urbana-Champaign, Urbana, IL 61801. { hnguyen6, zgahvari, haldar, minhdo, z-liang } @illinois.edu

although this could be easily generalized to accommodate more complicated lineshapes. Given the model (1), we are interested in analyzing CRBs on the metabolite amplitudes  $a_n(TE)$  as a function of TE.

### B. Cramér-Rao bound expressions

We assume the unknown parameters are the amplitudes, zero-order phase, and lineshape parameters, i.e.,

$$\boldsymbol{\theta} = \{a_1, \dots, a_N, \phi_0, r_1, \dots, r_N\}.$$

Cramér-Rao bound theory states that the variance of unbiased estimates is always lower bounded by

$$\text{var}(\hat{\theta}_k) \geq [\mathbf{F}^{-1}]_{kk}, \quad (5)$$

where  $\mathbf{F}$  is the Fisher information matrix [8].

We consider the context of additive complex Gaussian white noise  $\boldsymbol{\xi} \sim \mathcal{N}\{\mathbf{0}, \sigma^2 \mathbf{I}\}$ , for which the likelihood function  $L(\mathbf{y})$  of the noisy data  $\mathbf{y}$  can be easily expressed. Thus, each element of the Fisher information matrix can be computed as

$$\mathbf{F}_{\theta_i \theta_j} = E \left[ \left( \frac{\partial \ln L(\mathbf{y})}{\partial \theta_i} \right) \left( \frac{\partial \ln L(\mathbf{y})}{\partial \theta_j} \right)^T \right], \quad (6)$$

where the symbol  $E$  denotes the mean over the noise. One can further show that

$$\begin{aligned} \{\mathbf{F}\}_{a_i a_j} &= \frac{2}{\sigma^2} \text{Re} \left\{ \sum_{m=0}^{M-1} \varphi_{i,TE}^*[m] \psi_{i,r_i}^*[m] \right. \\ &\quad \left. \times \varphi_{j,TE}[m] \psi_{j,r_j}[m] \right\}. \end{aligned} \quad (7)$$

Other elements in the Fisher information matrix have similar expressions. Inverting the matrix  $\mathbf{F}$  gives the desired CRB matrix, with the first  $N$  diagonal elements being the CRBs on the amplitudes  $a_n$ , which are of interest in this work. Notice that the matrix entries depend on an inner product involving the basis functions and signal decay functions, which suggests that there can be interactions among metabolites.

### III. ANALYSIS OF TE SELECTION

We consider the following 17 MR-observable metabolites in the human brain [9], [10]: *aspartate*, *choline*, *creatine*, *ethanolamine*, *GABA*, *glucose*, *glutamate*, *glutamine*, *glutathione*, *histidine*, *homocarnosine*, *lactate*, *myo-inositol*, *N-acetylaspartate (NAA)*, *scyllo-inositol*, *taurine*, and *threonine*. For each metabolite, we simulate 1024 data points according to (1) at the magnetic field strength of 3T and spectral bandwidth of 1,200 Hz. Spectral parameters  $\alpha_{i,n}(TE)$ ,  $f_{i,n}(TE)$ , and  $\beta_{i,n}(TE)$  are obtained from quantum mechanical simulations of a spin-echo MR experiment [11]. Basis functions are then computed as in (3). Metabolite amplitudes,  $T_2$  values, and the lineshape parameter  $r_n$  are chosen to match reported values in the existing literature [10], [12]–[14]. For simplicity, we ignore the background signals originating from macromolecules and lipids.

The coefficient of variation, defined as the standard deviation of the estimated metabolite amplitude divided by its

mean, is a common metric used in the literature to express quality of parameter estimation. Thus, we consider the square root of the CRB, normalized by the metabolite amplitude, as a bound on the coefficient of variation. We denote this bound as the coefficient of variation bound (CVB). From the perspective of signal estimation, the desired TE is the one that has the smallest CVB, which in practice might lead to more accurate quantitation of metabolite concentrations.

### A. Simple case of one metabolite

To gain insight into the evolution of the CVB with TE, consider a reduced case where there exists only one spectral component, i.e.,  $N = 1$ . Due to decreased SNR at long TE, one might expect that as TE increases, the corresponding CVB increases. However, this is not true in general and it depends on how the metabolite profile changes with TE. The CRB on the amplitude can be reduced to the following compact form:

$$\begin{aligned} \text{CRB}_{a_1} &= \frac{\sigma^2}{2} \left( \sum_{m=0}^{M-1} |\varphi_{1,TE}[m]|^2 |\psi_1[m]|^2 \right. \\ &\quad \left. - \frac{(\sum_{m=1}^{M-1} m |\varphi_{1,TE}[m]|^2 |\psi_1[m]|^2)^2}{\sum_{m=1}^{M-1} m^2 |\varphi_{1,TE}[m]|^2 |\psi_1[m]|^2} \right)^{-1} \quad (8) \\ \text{CVB}_{a_1} &= \frac{\sqrt{\text{CRB}_{a_1}}}{c_1 e^{-TE/T_{2,1}}}. \end{aligned} \quad (9)$$

There are two factors affecting the change in the CVB as TE changes. The first factor is the term  $e^{-TE/T_{2,1}}$ , which shows that the CVB of the amplitude has an exponential dependence on TE. This factor comes from the inherent loss of signal at long TE. However, the second factor, which is the basis function  $\varphi_{1,TE}[m]$ , can offset the first factor by changing the three summation series involved in (8).

Fig. 1 shows CVBs of the amplitudes of NAA and lactate as a function of TE, together with their spectra at two representative TEs of 20 ms and 140 ms. The difference between the CVB curves of NAA and lactate is remarkable. In Figs. 1(c),(d) we observe that the CVB curve of NAA increases monotonically with TE, while the CVB curve of lactate does not. One possible explanation for this difference is that except for a decrease in amplitude, the NAA spectrum does not change shape as TE increases, while the lactate spectrum does, particularly in the region of 1.3 ppm. This experiment shows that even in the reduced case of one metabolite, an increase in TE does not necessarily increase the CVB. This behavior may not have been expected intuitively.

### B. Case of two metabolites

Spectral overlap is typically considered as a confounding problem in spectroscopy. To gain insight into the effect of the spectral overlap on the CVB, we consider the case of glutamate and glutamine. It is reported that a strong overlap of glutamate and glutamine resonances complicates their detection [10]. We compute the CVB on the amplitude of glutamate as a function of TE when glutamate is present in the spectrum alone and when glutamine is added to the spectrum, shown in Fig. 2(c). We observe that even when

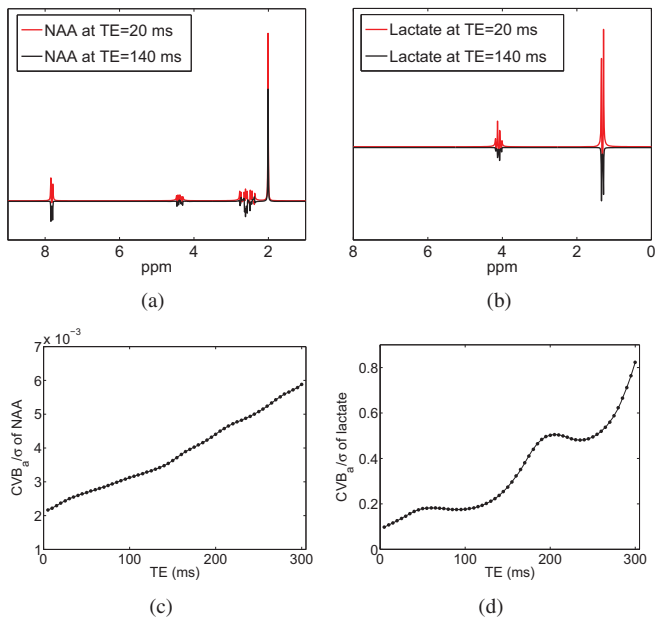


Fig. 1. The top row shows the change of the metabolite profiles with TE: (a) spectra of NAA at TE=20 ms (in red) and TE=140 ms (in black); (b) spectra of lactate at TE=20 ms (in red) and TE=140 ms (in black), shown in the same scale as (a). The bottom row shows the CVB on the amplitude of (c) N-acetylaspartate (NAA) and (d) lactate as a function of TE. The non-monotonic behavior of the CVB curve of lactate compared to NAA can be explained by the fact that the lactate spectrum changes significantly in the region of 1.3 ppm, while the NAA spectrum does not, except for a decrease in amplitude.

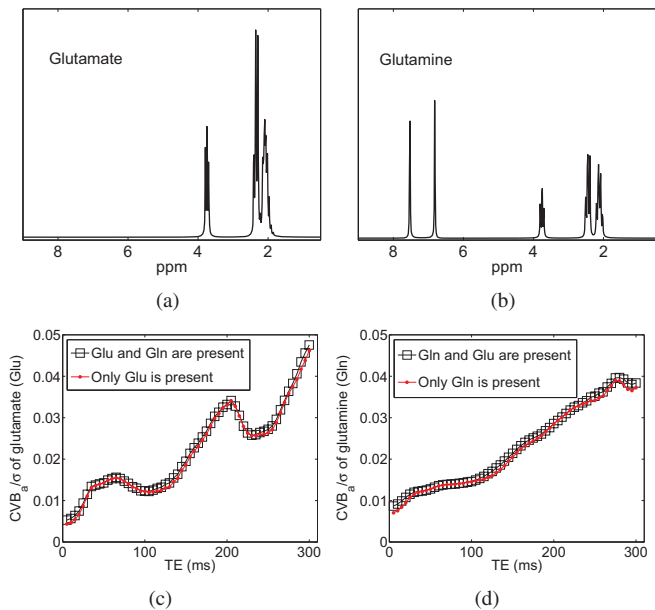


Fig. 2. The top row shows the spectra of (a) glutamate and (b) glutamine at TE=5 ms, both on the same scale. Spectral overlap is observed in the regions from 1.8 ppm to 2.6 ppm and from 3.5 ppm to 4 ppm. The bottom row shows (c) the CVB on the amplitude of glutamate in the presence (in black) and absence (in red) of glutamine; (d) the CVB on the amplitude of glutamine in the presence (in black) and absence (in red) of glutamate. In both cases, the CVB of one metabolite is not significantly affected by the presence of the other metabolite. This is not expected if judging intuitively from the observed spectral overlap.

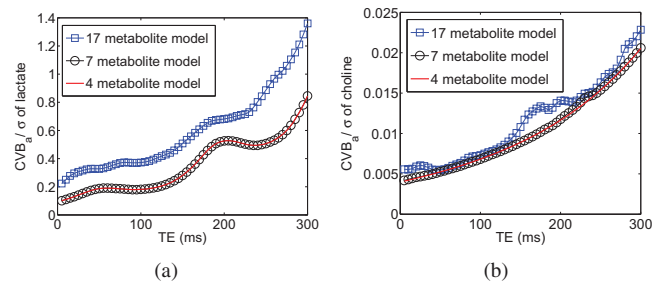


Fig. 3. CVB on the amplitude of (a) lactate and (b) choline in the case of regular (17 metabolites) and reduced (7 and 4 metabolites) models. The CVB curve decreases as the model order decreases. For clarity, this figure should be viewed in color.

there is overlap between these two metabolites, such as in the regions from 1.8 ppm to 2.6 ppm and from 3.5 ppm to 4 ppm (see Figs. 2(a),(b)), the CVB increases by a small factor ranging from 1.0 to 1.2 at different TEs. Similar CVB behavior is observed for the case when glutamine is present in the spectrum alone and when glutamate is added to the spectrum, shown in Fig. 2(d). Thus, the CVB plots show that overlaps in the spectra do not necessarily cause a large increment in the CVBs. From the CRB perspective, spectral overlap is not a significant obstacle for the quantitation of metabolite concentrations, unlike what visual intuition may suggest.

### C. General case of many metabolites

To gain insight into the CVB evolution as a function of TE in a more complete model, we consider a spectrum containing all of the 17 listed metabolites. In addition, to examine whether a reduced model order can lead to a further decrease in the CVB, we also consider two additional models. The first reduced model has 7 commonly reported metabolites that give rise to large signals at short TE: *NAA*, *choline*, *creatine*, *glutamate*, *glutamine*, *lactate*, and *myo-inositol* [9]. A further reduced model consists of 4 commonly observed metabolites that have long  $T_2$  values and contribute mainly to large signals at long TE: *NAA*, *choline*, *creatine*, and *lactate* [9].

Theoretically, it is clear that the reduced model describes the observed MR resonance process less accurately than the original model with more metabolites. In practice though, any loss of accuracy of the reduced model decreases at longer TE, because the signal contribution from metabolites with short  $T_2$  becomes very small. However, the exact value of TE at which we can reliably assume a reduced model is still an open question and needs future investigation.

Figure 3 shows CVBs of the amplitude of lactate and choline for the original model with 17 metabolites, the reduced model with 7 metabolites, and the reduced model with 4 metabolites. In the cases of both lactate and choline, we see that reducing the model order from 17 to 7 metabolites yields a smaller CVB at each TE. This confirms that the decreased correlation between metabolites lowers the CRB, and hence, the CVB. However, further reducing the model order from 7 to 4 metabolites does not yield a noticeable

improvement, as can be seen from Fig. 3. Assuming we know the value of TE at which the reduced model is reasonable, we can tell from the corresponding CVB plots whether using the reduced model with prolonged TE could yield a smaller CVB compared to the original model at short TE. Notice that because the CVB curves tend to increase as TE increases, the CVB criteria suggests that excessively long TE values should not be chosen even when using the reduced model.

In this discussion, we have ignored the presence of background signals. When these signals are included, we expect the CVB will increase further at short TE. Because background signals decay quickly as TE prolongs, their inclusion would potentially favor the choice of longer TEs.

#### IV. CONCLUSIONS

In proton MR spectroscopy, echo time (TE) is a crucial parameter that influences the appearance of the observed spectrum. In this work, we provided a quantitative analysis of the effect of different TE values. Specifically, based on estimation theory, we use the CRB to compute a bound on the coefficient of variation of the unknown spectral amplitudes as a function of TE. We showed that the form of the spectral basis functions and their interactions through inner products play important roles on the achievable estimation performance. We also observed that the use of a reduced model, with a smaller number of metabolites at long TE, may or may not yield a reduction of the CVB compared to the regular model at short TE. The relative performance of different models depends on the metabolite of interest, and the range of TEs at which each model can be reliably assumed. Unlike empirical studies, which face practical limitations on acquisition time, this CRB analysis enables easy evaluation of an arbitrarily large range of TEs.

#### V. ACKNOWLEDGEMENTS

We would like to thank Brian J. Soher for providing the GAVA spectral simulation software package.

#### REFERENCES

- [1] R. Kreis, "Quantitative localized  $^1\text{H}$  MR spectroscopy for clinical use," *J. Prog. NMR Spect.*, vol. 31, pp. 155–195, 1997.
- [2] D. J. O. McIntyre, R. A. Charlton, H. S. Markus, and F. A. Howe, "Long and short echo time proton magnetic resonance spectroscopic imaging of the healthy aging brain," *J. Magn. Reson. Imag.*, vol. 26, pp. 1596–1606, 2007.
- [3] M. Inglese, M. Spindler, J. S. Babb, P. Sunenshine, M. Law, and O. Gonen, "Field, coil, and echo-time influence on sensitivity and reproducibility of brain proton MR spectroscopy," *Am. J. Neuroradiol.*, vol. 27, pp. 684–688, Mar 2006.
- [4] I. Marshall, J. Wardlaw, C. Graham, L. Murray, and A. Blane, "Repeatability of long and short echo-time in vivo proton chemical-shift imaging," *Neuroradiol.*, vol. 44, pp. 973–980, 2002.
- [5] S. Cavassila, S. Deval, C. Huegen, D. van Ormondt, and D. Graveron-Demilly, "Cramer-Rao bound expressions for parametric estimation of overlapping peaks: influence of prior knowledge," *J. Magn. Reson.*, vol. 143, pp. 311–320, 2000.
- [6] —, "Cramer-Rao bounds: an evaluation tool for quantitation," *NMR Biomed.*, vol. 14, pp. 278–283, 2001.
- [7] S. W. Provencher, "Estimation of metabolite concentrations from localized in vivo proton NMR spectra," *Magn. Reson. Med.*, vol. 30, pp. 672–679, 1993.
- [8] S. M. Kay, *Fundamentals of Statistical Signal Processing: Estimation Theory*. Englewood Cliffs, NJ: Prentice-Hall, 1993.

- [9] P. B. Barker and D. D. M. Lin, "In vivo proton MR spectroscopy of the human brain," *Prog. NMR Spect.*, vol. 49, pp. 99–128, 2006.
- [10] V. Govindaraju, K. Young, and A. A. Maudsley, "Proton NMR chemical shifts and coupling constants for brain metabolites," *NMR Biomed.*, vol. 13, pp. 129–153, 2000.
- [11] B. J. Soher, K. Young, A. Bernstein, Z. Aygula, and A. A. Maudsley, "GAVA: Spectral simulation for in vivo MRS applications," *J. Magn. Reson.*, vol. 185, pp. 291–299, 2007.
- [12] F. Traber, W. Block, R. Lamerichs, J. Gieseke, and H. H. Schild, " $^1\text{H}$  metabolite relaxation times at 3.0 Tesla: measurements of T1 and T2 values in normal brain and determination of regional differences in transverse relaxation," *J. Magn. Reson. Imag.*, vol. 19, pp. 537–545, 2004.
- [13] C. Choi, N. J. Coupland, P. P. Bhardwaj, S. Kalra, C. A. Casault, K. Reid, and P. S. Allen, " $T_2$  measurement and quantification of glutamate in human brain in vivo," *Magn. Reson. Med.*, vol. 56, pp. 971–977, 2006.
- [14] P. B. Barker, D. O. Hearshen, and M. D. Boska, "Single-voxel proton MRS of the human brain at 1.5T and 3.0T," *Magn. Reson. Med.*, vol. 45, pp. 765–769, 2001.